

1-P
NATIONAL AERONAUTICS AND SPACE ADMINISTRATION

Technical Memorandum 33-597

*Postoperational Examination of an Externally
Configured Thermionic Converter*

W. M. Phillips

(NASA-CR-131523) POSTOPERATIONAL
EXAMINATION OF AN EXTERNALLY CONFIGURED
THERMIONIC CONVERTER (Jet Propulsion Lab.)
19 p HC \$3.00
CSCL 18I
N73-21560
Unclas
G3/22 68285

JET PROPULSION LABORATORY
CALIFORNIA INSTITUTE OF TECHNOLOGY
PASADENA, CALIFORNIA

March 15, 1973

18

1. Report No. 33-597	2. Government Accession No.	3. Recipient's Catalog No.	
4. Title and Subtitle POSTOPERATIONAL EXAMINATION OF AN EXTERNALLY CONFIGURED THERMIONIC CONVERTER		5. Report Date March 15, 1973	
		6. Performing Organization Code	
7. Author(s) W. M. Phillips		8. Performing Organization Report No.	
9. Performing Organization Name and Address JET PROPULSION LABORATORY California Institute of Technology 4800 Oak Grove Drive Pasadena, California 91103		10. Work Unit No.	
		11. Contract or Grant No. NAS 7-100	
12. Sponsoring Agency Name and Address NATIONAL AERONAUTICS AND SPACE ADMINISTRATION Washington, D.C. 20546		13. Type of Report and Period Covered Technical Memorandum	
		14. Sponsoring Agency Code	
15. Supplementary Notes			
16. Abstract <p>An externally configured thermionic converter was operated for 200 h. The converter was disassembled and examined to determine internal changes as a result of operation. The metal/ceramic seals and all joints were unaffected by operation. Converter output voltage and operational time were sufficient to produce electrolysis of stabilized zirconia spacers used in the converter.</p> <p>Surface analysis of the electrode surfaces indicated the presence on the tungsten emitter of only oxygen, carbon, and silicon. The niobium collector was, however, 25 to 40% covered with other elements. This coverage represented all elements present within the converter as construction materials other than silicon and tungsten, which were not detected on the collector, and carbon, which was detected only in small amounts.</p> <p style="text-align: center;">Details of illustrations in this document may be better studied on microfiche</p>			
17. Key Words (Selected by Author(s)) Power Sources Test Facilities and Equipment		18. Distribution Statement Unclassified -- Unlimited	
19. Security Classif. (of this report) Unclassified	20. Security Classif. (of this page) Unclassified	21. No. of Pages 15	22. Price

NATIONAL AERONAUTICS AND SPACE ADMINISTRATION

Technical Memorandum 33-597

*Postoperational Examination of an Externally
Configured Thermionic Converter*

W. M. Phillips

JET PROPULSION LABORATORY
CALIFORNIA INSTITUTE OF TECHNOLOGY
PASADENA, CALIFORNIA

March 15, 1973

PREFACE

The work described in this report was performed by the Propulsion Division of the Jet Propulsion Laboratory.

CONTENTS

I.	Introduction	1
II.	Externally Configured Converter Design	1
III.	Converter Electrical Parametric Tests	2
IV.	Postoperational Examination	3
V.	Summary and Conclusions	6
	References	7

TABLE

1.	Ion scattering spectrometric surface analysis results	9
----	---	---

FIGURES

1.	Cross section of externally configured converter design	10
2.	Static current voltage curves for the externally configured converter	11
3.	Zirconia insulator spacer ring after operation	11
4.	Niobium collector beneath zirconia insulator ring showing cracking as a result of oxygen transfer produced by electrolysis	12
5.	Helium gas gap surface of collector showing second phase produced by helium impurities	12
6.	Emitter surface opposite zirconia spacer rings showing grain boundary texturing of surface	13
7.	Tungsten emitter to niobium emitter flange meId joint back-brazed with vanadium	14
8.	Alumina-to-niobium metal/ceramic seal	14

Preceding page blank

ABSTRACT

An externally configured thermionic converter was operated for 200 h. The converter was disassembled and examined to determine internal changes as a result of operation. The metal/ceramic seals and all joints were unaffected by operation. Converter output voltage and operational time were sufficient to produce electrolysis of stabilized zirconia spacers used in the converter.

Surface analysis of the electrode surfaces indicated the presence on the tungsten emitter of only oxygen, carbon, and silicon. The niobium collector was, however, 25 to 40% covered with other elements. This coverage represented all elements present within the converter as construction materials other than silicon and tungsten, which were not detected on the collector, and carbon, which was detected only in small amounts.

I. INTRODUCTION

An externally configured thermionic converter is one concept that is being investigated as a possible thermionic fuel element for an advanced in-core thermionic reactor. To help evaluate the externally configured concept, an unfueled thermionic converter was parametrically tested by electrical heating at the Jet Propulsion Laboratory (JPL). The converter was designed and fabricated by Thermo Electron Corporation (TECO), Waltham, Massachusetts, in accordance with JPL specifications and design requirements.

During the parametric tests, the static, dynamic, and other operational characteristics that are unique to this externally configured thermionic converter were investigated. After termination of parametric testing, the converter was examined to evaluate any changes in the condition of the device.

II. EXTERNALLY CONFIGURED CONVERTER DESIGN

A cross section of the converter design is shown in Fig. 1. The emitting surface of the CVD fluoride tungsten emitter was 1.143 cm (0.450 in.) in diameter by 25.4 cm (10 in.) long. The emitter active electrode area was 84 cm². The outer diameter of the tungsten emitter was 2.03 cm (0.8 in.) giving a wall thickness of 0.44 cm (0.175 in.). The active emitting surface of the emitter was chemically etched for 15 min. with equal volumes of 5% sodium hydroxide and saturated potassium ferricyanide. The electrical leads were 0.1-cm (0.040-in.) thick tungsten cylindrical extensions of the emitter body that were brazed to niobium flanges. The niobium flanges served as the emitter electrical connections and mechanical supports. Enclosed within the niobium emitter flanges were alumina spacer rings to maintain interelectrode spacing.

The niobium 1%-zirconium collector was 1.093-cm (0.430-in.) outer diameter by 0.635-cm (0.250-in.) inner diameter. The active collector surface was coated with a few microns of molybdenum that were condensed on the collector from a molybdenum filament. The collector had three yttria-stabilized, zirconia cylindrical inserts evenly spaced axially along the collector surface. The insulating zirconia inserts were provided to reduce the possibility of emitter collector shorts.

A niobium 1%-zirconium flange was welded (at both ends) to the collector. A copper birdcage was brazed to each niobium collector flange, both of which served as a flexible, electrical collector lead and mechanical support. The collector was cooled by water through a variable conductance, 0.014-cm (0.007-in.) gas gap. Trim heaters were attached to the collector leads to compensate for heat losses. The collector flange and emitter flange were electrically and thermally separated by a niobium-welded bellows and a niobium-alumina metal/ceramic seal assembly. This bellows-insulator assembly was welded to both emitter and collector flanges to seal the cesium space.

III. CONVERTER ELECTRICAL PARAMETRIC TESTS

The emitter was electrically heated with an RF induction coil. The RF coil was shaped to compensate for end thermal losses and to flatten the temperature distribution (Ref. 1). Emitter temperatures were determined with an optical pyrometer, using black body holes in the emitter and surface brightness measurements.

Static current-voltage curves at nominal temperatures of 1800 K, 1900 K, and 2000 K were determined by TECO (Ref. 2) as an acceptance test prior to delivery to JPL. The TECO current-voltage curves (with collector and cesium temperatures optimized) are shown in Fig. 2. The emitter temperature for each current-voltage curve was defined as the maximum observed temperature. The maximum emitter temperature occurred at the midplane of the converter; axial temperature gradients ranged from a few degrees to a maximum of 150°C at one end.

After completion of acceptance testing at TECO, the converter was shipped to JPL. Dynamic and static current-voltage curves were determined

(Ref. 3). The static current-voltage curves measured at JPL are also shown in Fig. 2. The maximum converter output power, which was limited by input power from the RF induction heater, was 178 W (1.95 W/cm^2) at an emitter temperature of 1946 K. The conversion efficiency was calculated from calorimetry to be 5.5%. The converter power output obtained at JPL at the same temperatures was markedly lower than those obtained by TECO. The possible causes for this are discussed in Section IV.

The data indicated the importance of emitter temperature flattening on converter performance. The converter output power was increased 25% when the temperature distribution was $1860 \pm 0 - 60 \text{ K}$ instead of $1860 \pm 20 - 160 \text{ K}$. The converter output was slow to respond to changes in cesium pressure and collector temperature. This suggested a possible contamination of either the emitter or collector surface and a cause for the low performance.

Plugging of the water coolant line caused premature termination of the test after 190 h. During the 190 h of operation the converter itself maintained its integrity and withstood 46 controlled shutdowns and approximately 13 abrupt shutdowns.

IV. POSTOPERATIONAL EXAMINATION

Attempts to remove the hard water deposits from the converter water coolant line were unsuccessful. The converter was, therefore, disassembled to determine the cause of the low performance after the initial acceptance test, which was high performance.

The cause of the low performance became apparent after disassembly. The zirconia insulators (inserts in the collector) were blackened and cracked as shown in Fig. 3. The effect is attributed to electrolysis of the zirconia.

Electrolytic characteristics of oxides have been documented in a number of investigations (Refs. 4, 5, and 6). In the case of $\text{Y}_2\text{O}_3\text{-ZrO}_2$ the conductivity is attributed to oxygen-ion mobility in the defect solid solution. The defects are oxygen vacancies created to produce lattice neutrality when Y^{+3} ions are substituted for Zr^{+4} ions in the fluoride-type structure of the $\text{Y}_2\text{O}_3\text{-ZrO}_2$ solid solution.

$\text{Y}_2\text{O}_3\text{-ZrO}_2$ specimens have been tested in air at 1673 K with an applied electrical potential (Ref. 7). In this experiment, up to 3 V were applied to the test specimen for periods of up to 159 h, producing currents of up to 5 A/cm². As electrolysis proceeded, the Zr^{+4} ions present in the ZrO_2 were reduced to the divalent state with the formation of zirconium monoxide or black zircon (ZrO). In contrast to the starting material, the ZrO had a much higher electrical conductivity.

Similar electrolysis has been observed in aluminum oxide (Al_2O_3) at 1473 K, however, longer times (5313 h vs 159 h) and higher voltages (100 V vs ≤ 3 V) were needed to produce damage to the ceramic (Ref. 8).

Literature values for resistivity of zirconia at the collector operating temperature of 900 K are in the range of 2000 $\Omega\text{-cm}$ (Refs. 9 and 10). This results in a resistance of approximately 500 Ω for each of the zirconia insulator inserts. A diode potential of 1 V would produce a current density of 0.0025 A/cm². This is well below the current density needed to produce damage in other experiments (Ref. 7) in similar test times. Since the insulators were only in physical contact with the collector and not well-bonded to the collector, and since thermal conductivity of the insulator is low, it is probable that outer portions of the insulators were operating at temperatures much closer to the emitter temperature (up to 2000 K). Thus, they had lower resistivity and conducted the increased currents needed to produce the damage observed.

The production of black zirconium-oxide (ZrO) from zirconia (ZrO_2) would leave free oxygen to transfer to the niobium collector where it would produce oxide precipitates and cracking beneath the insulator groove, as shown in Fig. 4. The inner surface of the collector, which was one of the helium heat transfer gas gap surfaces, showed reaction layers that were attributed to impurities in the helium gas (Fig. 5). This is external to the thermionic conversion surfaces and did not affect converter performance.

The emitting surface was clean and shiny. The only evidence of operation was a slight texturing of the surface opposite the three zirconia insulating rings. A metallographic section of the emitter surface opposite a zirconia ring is shown in Fig. 6. This photomicrograph indicates that the texturing was due to a very slight grain boundary attack.

Examination of the weld joint between the tungsten emitter and the niobium flange (Fig. 7), which was back-brazed with vanadium, indicated the joint to be sound, without any signs of porosity or cracking.

The metal/ceramic seal, in which the alumina was metallized and copper-brazed to niobium, was in excellent condition and unaffected by converter operation, and is shown in Fig. 8.

Ion scattering spectrometric analyses were run on:

- (1) The emitter surface opposite one of the ZrO_2 spacer rings.
- (2) The collector surface adjacent to one ZrO_2 spacer ring.
- (3) The collector surface beneath one ZrO_2 spacer ring.

The results are shown in Table 1. Ion scattering, spectrometric techniques provided surface analyses to depths of several monolayers.

Essentially, all impurities have evaporated or sublimed from the emitter with the exception of silicon, oxygen, and carbon. Both the carbon and oxygen levels appear to be in excess of that which is in solution at the operating temperature of the emitter (solubility limits are approximately 10 ppm carbon and 50 ppm oxygen at 1650°C) (Refs. 11 and 12). Neither of these impurities appear associated with cesium, since cesium concentration is low on the emitter surface.

Carbon has been observed as a common surface impurity on tungsten (Refs. 13 and 14). In these vacuum work function tests, the carbon has been removed by a high temperature (1900 K) exposure to a low partial pressure of oxygen ($7 \times 10^{-5} \text{ N/m}^2$ (5×10^{-7} torr)). Thus, in the closed system of a sealed thermionic converter, carbon is not readily removed from the emitter surface, as it was in the above open-ended pumped vacuum system conditions.

The amount of oxygen present on the emitter indicates that it is present as an oxide. Tungsten oxides have been identified on both the emitter and collector surfaces (Ref. 14) in vacuum work function tests. Under the vacuum work function measurement conditions, these oxides were readily transferred from the emitter to the collector at normal emitter temperatures. The analyses of the electrode surfaces indicate the presence of oxygen on both emitter and collector; however, tungsten was not detected on the collector

surface. Thus, the results of these analyses indicate that oxygen and carbon do not transfer as readily from the emitter to the collector as might be predicted. The prediction is based on free energies of tungsten compounds at emitter temperatures and free energies of niobium compounds at collector temperatures. The only element appearing on the emitter surface in greater amounts than on the collector was silicon. Because of the high solubility of silicon in tungsten (~5 wt% at emitter temperatures) (Ref. 15), all of the detected silicon is believed to be in solution.

The collector analyses appear to be a scan of the periodic table with practically all elements, which were present in the converter, present as impurities on the collector surface. The surface was estimated to be 25 to 40% covered with contaminants, with the remaining 60 to 75% being niobium. The most unexpected result of the collector analysis was the absence of tungsten and the small concentration of carbon on the collector surface. It must be kept in mind that the total operating time of the thermionic converter was 200 h. Thus, transfer of tungsten and carbon from the emitter to the collector may occur at longer times, but transfer is definitely not rapid. The high carbon concentration beneath the ZrO_2 insulator suggests contamination during machining or during installation of the ZrO_2 insulators into the collector subassembly. The high rhenium concentration, coupled with ZrO_2 resistivity degradation, suggests that the ZrO_2 spacer rings were heated by current flowing through the rhenium wires through the ZrO_2 to the niobium collector. The rhenium wires were used to hold the ZrO_2 in the collector slots and to prevent direct contact between ZrO_2 spacer rings and emitter.

Scans at greater depths into the converter surface indicated that aluminum disappeared at approximately 40 monolayers, indicating it to be from the alumina insulators rather than the niobium impurity. Fluorine was detected in the fluoride-vapor-deposited tungsten emitter, but it was very erratic. This indicates the fluorine to be present in bubbles rather than as a continuous dispersion.

V. SUMMARY AND CONCLUSIONS

Approximately 200 h of operation of the thermionic converter was sufficient to produce electrolysis of the zirconia insulator spacer rings, which reduced the electrical output of the converter, both by electrical shorting

and contamination of the collector surface. Surface analyses of the electrode surfaces indicated that only carbon, oxygen, and silicon remained on the tungsten emitter surface in significant amounts. The niobium collector surface was 25 to 40% covered with other elements transferred from other portions of the converter. These elements are all present within the converter, with three significant exceptions: tungsten and silicon, which were not detected on the collector, and carbon, which was present on the collector in amounts far below levels present on the emitter.

REFERENCES

1. Schock, A., "Analysis and Optimization of "Full Length" Diodes, " in the proceedings of the Second International Thermionic Electrical Power Generation Symposium, Stresa, Italy, May 27-31, 1968, Euratom Center for Information and Documentation, pp. 865-878.
2. Ernst, D. M., "Design, Fabrication, and Testing of Externally Configured Thermionic Diodes, " in the proceedings for the IEEE Conference Record of 1970 Thermionic Conversion Specialist Conference, Miami Beach, Fla., pp. 533-538, Oct. 1970.
3. Shimada, K., et al., Parametric Testing of an Externally Configured Thermionic Converter, Technical Memorandum 33-504, Jet Propulsion Laboratory, Pasadena, Calif., Nov. 1971.
4. Manning, J. R., "Diffusion on Ionic Conductivity: Kinetic Theory, " in Mass Transport in Oxides, NBS Special Publication 296, pp. 53-63, 1968.
5. Bray, D. T., and Merten, U., "Transport Numbers in Stabilized Zirconia, " J. Electrochem Soc., Vol. 3, No. 4, pp. 447-452, 1963.
6. Pappis, J., and Kingery, W. D., "Electrical Properties of Single-Crystal and Polycrystalline Alumina at High Temperatures, " J. Am. Ceramic Soc., Vol. 44, No. 9, pp. 459-464, 1961.
7. Golchshtein, Y. P., and Safonov, A. A., "Current Density through the Electrodes of a MHD Generator Made of $ZrO_2-Y_2O_3$ Ceramic, " Teplogizika Vysokilch Temperature, Vol. 8, No. 2, pp. 398-402, March-April, 1970, Translated by Consultants Bureau, Plenum Pub. Corp., New York, N. Y.
8. Chin, J., and Messick, C. W., "Thermal Stability Testing of an Electrically Loaded Sheath Insulator, " in the proceedings for the IEEE 1969 Thermionic Conversion Specialists Conference, Oct. 21-23, 1969, Carmel, Calif., pp. 394-403.

REFERENCES (contd)

9. Thorpe, J. S., et al., "Electron Spin Resonance in Single Crystal Yttria Stabilized Zirconia," J. Mater. Sci., Vol. 7, pp. 729-734, 1972.
10. Kesler, G. H., "Thermal Insulation," in High Temperature Materials and Technology, p. 700. Edited by Campbell and Sherwood. John Wiley and Sons, Inc., New York, N. Y., 1967.
11. Goldschmidt, H. J., and Brand, J. A., "The Tungsten-Rich Regions of the System Tungsten-Carbon," J. Less Common Metals, Vol. 5, pp. 181-194, 1963.
12. Klopp, W. D., and Barth, V. D., Diffusion Rates and Solubilities of Interstitials in Refractory Metals, DMIC Memorandum No. 50, Apr. 1960.
13. Alleau, T., and Bacal, M., "Influence of Oxygen Absorption and Oxygen-Cesium Co-Adsorption on (100) Tungsten Work Function," in the proceedings for the IEEE 1970 Thermionic Conversion Specialists Conference, Oct. 26-29, 1970, Miami Beach, Fla., pp. 434-440.
14. Lieb, D., and Rufeh, F., "The Utilization of Tungsten Oxides for Additive Thermionic Converters," in the proceedings of the 3rd International Conference on Thermionic Electrical Power Generation, Julich, Germany, June 5-9, 1972, Paper F46.

Table 1. Ion scattering spectrometric surface analysis results

Element	Approximate concentration ^a		
	Emitter	Collector surface	Collector beneath spacer
Tungsten	Large	N. D.	N. D.
Rhenium	Low	Large	Medium
Cesium	Low	Large	Large
Oxygen	Large	Large	Large
Carbon	Medium	Low	Medium/large
Aluminum	N. D.	Large	Medium
Copper	N. D.	Medium	N. D.
Nickel	Low	Medium	Medium
Silicon	Medium	N. D.	N. D.
Titanium	N. D.	Medium	N. D.
Vanadium	N. D.	Medium	N. D.
Zirconium	Low	Medium	Medium

^aN. D. = not detected < ~ 1%

Low = 1% range

Medium = 3-5% range

Large = > ~ 5%

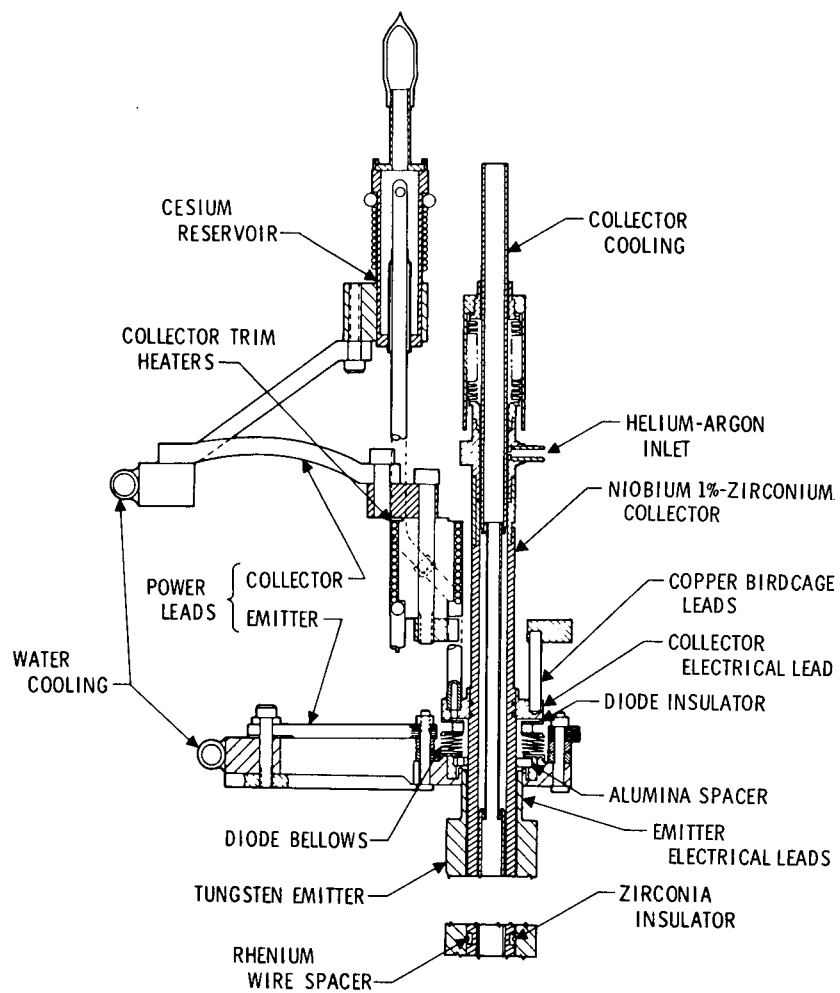
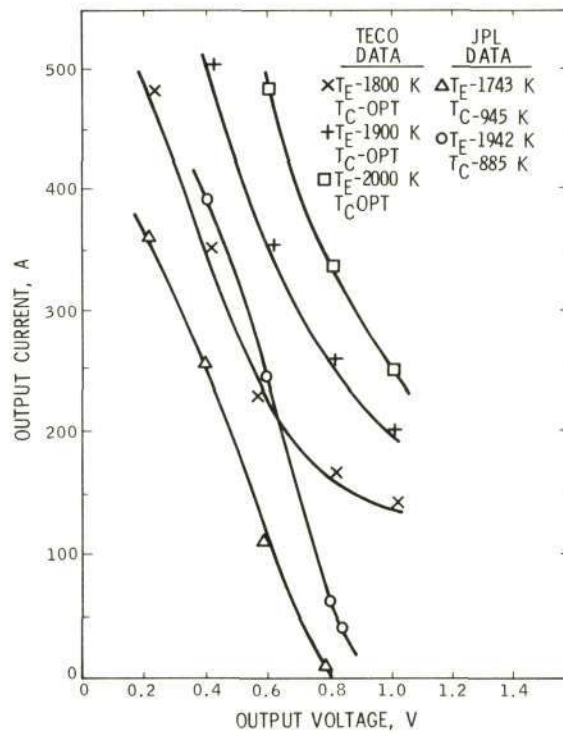


Fig. 1. Cross section of externally configured converter design



Reproduced from
best available copy.

Fig. 2. Static current voltage curves for the externally configured converter

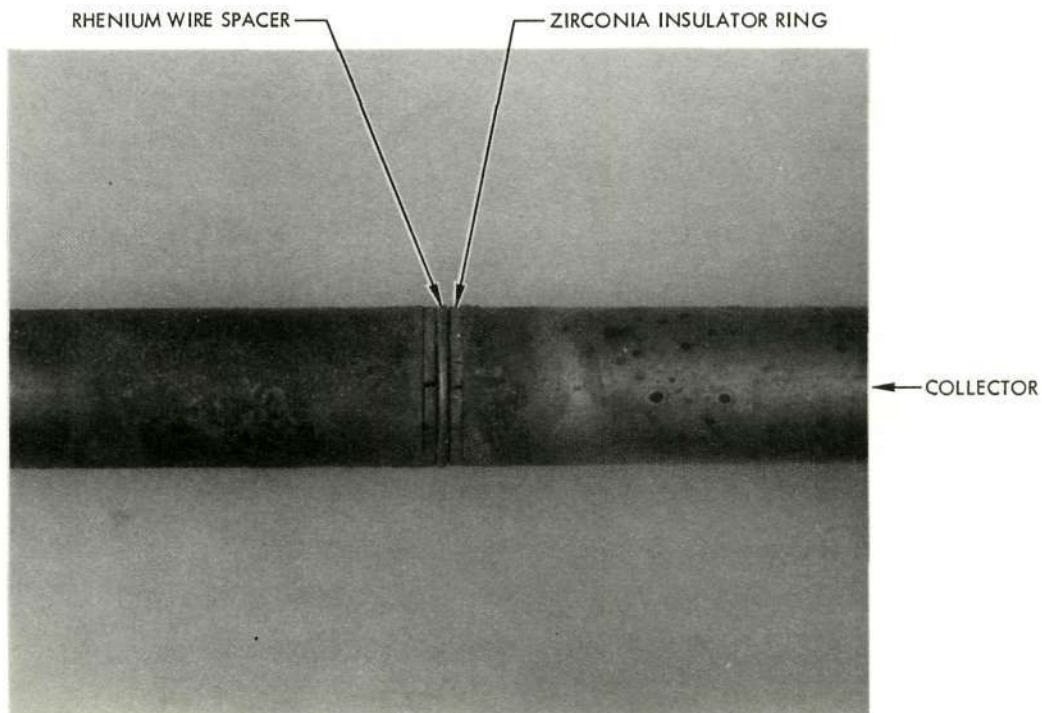


Fig. 3. Zirconia insulator spacer ring after operation

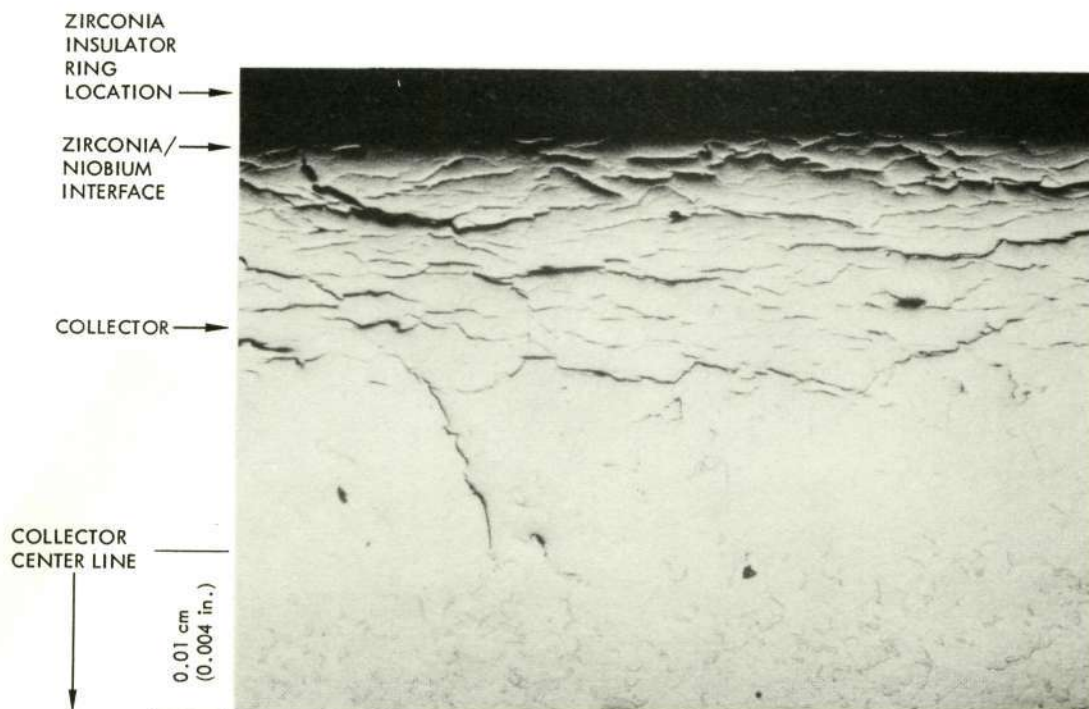


Fig. 4. Niobium collector beneath zirconia insulator ring showing cracking as a result of oxygen transfer produced by electrolysis



Fig. 5. Helium gas gap surface of collector showing second phase produced by helium impurities

Reproduced from
best available copy.

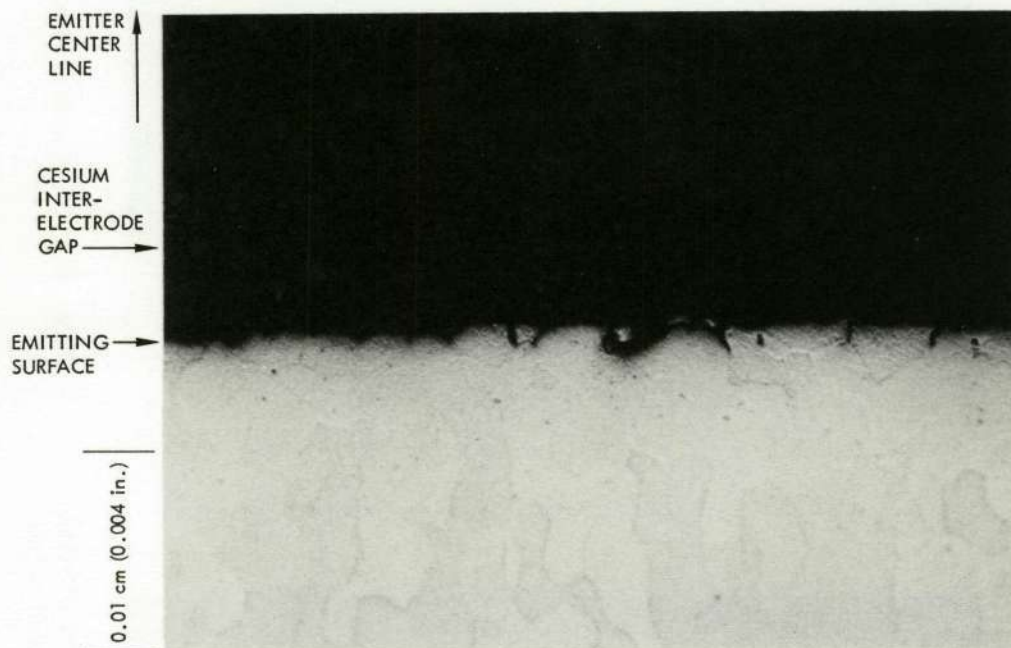


Fig. 6. Emitter surface opposite zirconia spacer rings showing grain boundary texturing of surface

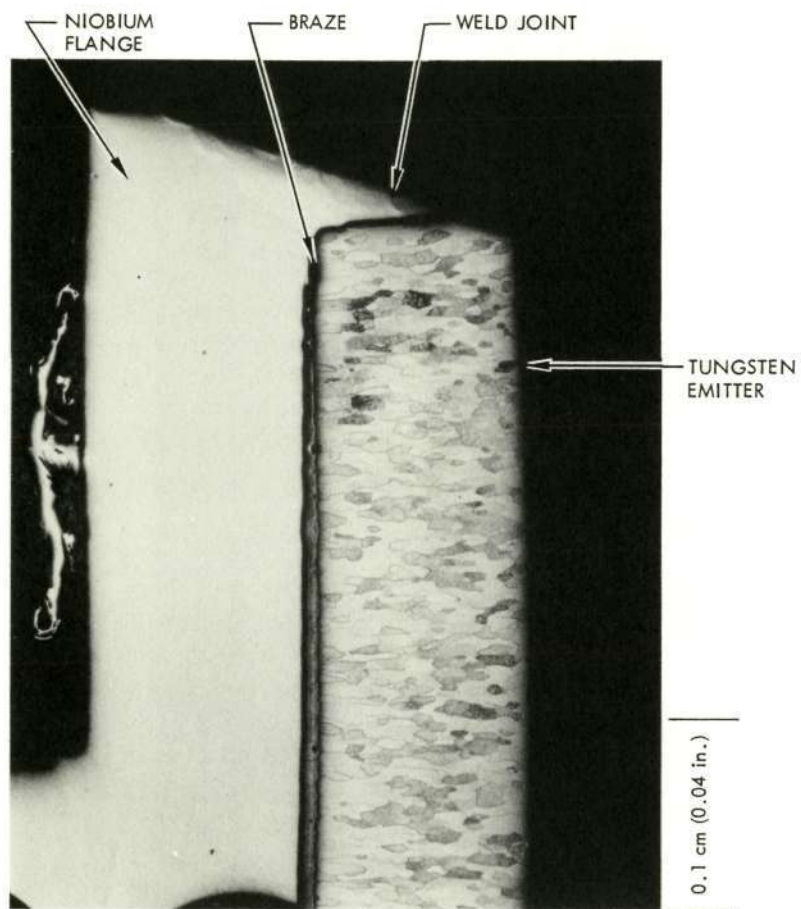


Fig. 7. Tungsten emitter to niobium emitter flange weld joint back-brazed with vanadium

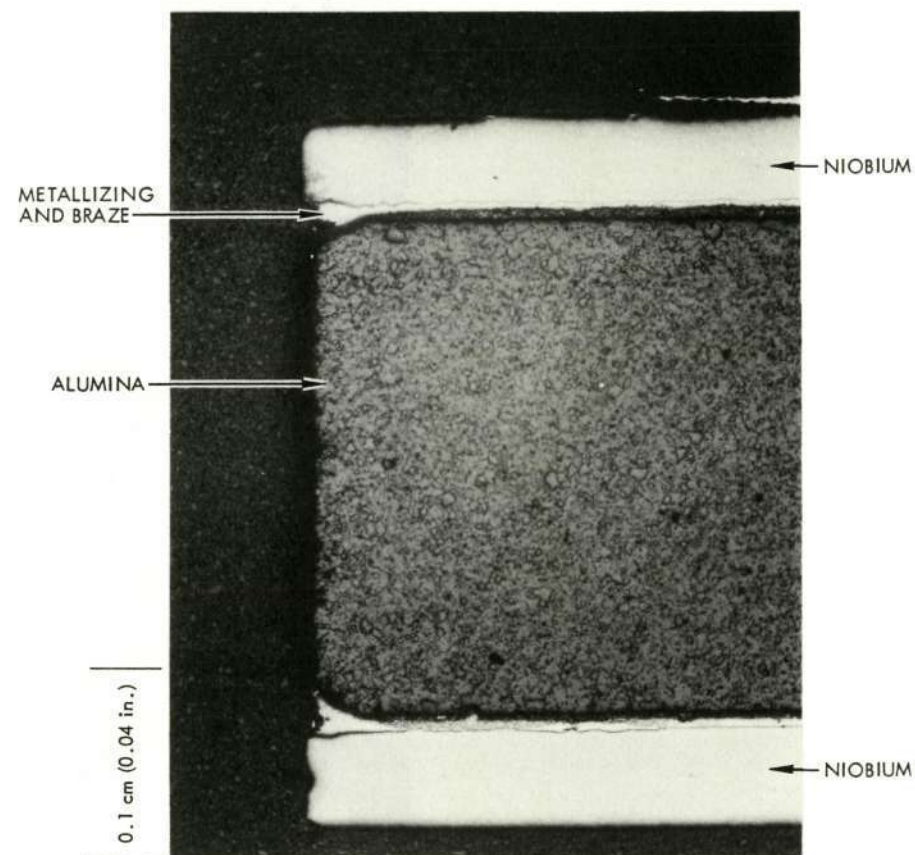


Fig. 8. Alumina-to-niobium metal/ceramic seal